Recent advances in understanding substorm dynamics

V. A. Sergeev,[1] V. Angelopoulos,[2] and R. Nakamura[3]

Received 5 January 2012; revised 7 February 2012; accepted 8 February 2012; published 6 March 2012.

[1] Magnetospheric substorms are elemental processes of solar wind energy storage and explosive release in Earth's magnetosphere. They encompass fundamental plasma physics questions, are ubiquitous during all types of geomagnetic conditions, contribute significantly to magnetic storms, and are a key element of Space Weather applications. This paper reviews recent major advances enabled by modern multi-point space-based and ground-based platforms. These datasets have also empowered a system-wide perspective and advanced modeling. We particularly highlight progress in two areas: (1) substorm onset timing and evidence for current sheet preconditioning and destabilization and (2) fast flows and dipolarizations, including the role of entropy in magnetotail plasma propagation. **Citation:** Sergeev, V. A., V. Angelopoulos, and R. Nakamura (2012), Recent advances in understanding substorm dynamics, *Geophys. Res. Lett.*, *39*, L05101, doi:10.1029/2012GL050859.

1. Introduction

[2] Sparse spacecraft coverage of the vast, dynamic magnetotail has been a source of many interpretational difficulties and much controversy regarding substorm processes. Progress in key areas of substorm studies has been made recently due to multi-point observations by Cluster and especially the Time History of Events and Macroscale Interactions during Substorms (THEMIS) mission, which also provided an expanded network of ground observatories. Global MHD simulations, especially when closely coordinated with such multi-point observations, have helped interpret a complicated, dynamic, truly three-dimensional plasma configuration. When available, dynamically-adaptive data-based magnetospheric models have also improved the mapping of slowly time-varying configurations. The extended operation of ISTP spacecraft (Geotail, Polar, Wind) have made possible both concurrent monitoring with Cluster and THEMIS and a large database facilitating advanced statistical studies. The combination of these tools has resulted in considerable progress in our understanding of substorm-related phenomena (evidenced by several hundred papers since the start of the THEMIS active phase reviewed in our paper), with the most notable advances in the two key areas detailed below.

[1]Earth Physics Department, St. Petersburg State University, St. Petersburg, Russia.
[2]Department of Earth and Space Sciences and Institute of Geophysics and Space Physics, University of California, Los Angeles, California, USA.
[3]Space Research Institute, Austrian Academy of Sciences, Graz, Austria.

0094-8276/12/2012GL050859

2. Substorm Onset Timing and Location

[3] Substorm onset, manifested as rapid brightening, breakup, and poleward expansion of the aurora, is characterized by explosive development of dissipative processes starting from a localized part of the plasma sheet and resulting in fast flows, plasma heating, and particle precipitation. Within several minutes, significant tail reconfiguration takes place. Understanding the sequence of key processes leading to substorm onset has been a long-standing, critical question in near-Earth space plasma physics. Auroral observations were considered the most accurate way of timing and locating explosive onset signatures (note, however, limitations inherent in mapping, discussed in 2.3.2, and ionospheric dynamics, taken up in section 2.3.3).

[4] Even though the network of ground observatories has been expanded, proper organization of observations made by a sparse network of satellites requires simple interpretational scenarios. In the past, onset signatures were thought to be produced by one of two processes: magnetic reconnection (MR) or current disruption (CD, some current-driven instability). Based on previous statistical results, these processes have been associated with spatially separated domains (MR at 20–30 Re and CD at approximately <10–10 Re) with their possible sequences named *'In → Out'*, or *'Out → In'* according to nominal distance and propagation direction. Such an association may not always be valid, however; also it often may be impossible to distinguish magnetic reconnection from current disruption. Therefore, establishing and validating an interpretative phenomenological model of the primary changes in the magnetotail at substorm onset is critical to focus concerted attention on the primary physics at play.

2.1. Global Pattern of Plasma Sheet Changes

[5] Analyses of the magnetotail response during substorms using the vast Geotail database (3787 substorm onsets, as determined by global imagers over 10 years and complemented by Polar and GOES measurements) organized in time relative to onset have revealed the major features of explosive tail plasma sheet reconfiguration [*Machida et al.*, 2009; *Miyashita et al.*, 2009]. Although limited to 2 min time resolution and around 5 Re spatial resolution, these results confirm that a statistically significant plasma sheet perturbation starts at around 18 Re from Earth near the tail center, where the cross-tail convection electric field increases sharply (indicating enhanced plasma transport and dissipation), and the total pressure decreases sharply (signifying unloading of lobe magnetic flux). This perturbation is accompanied by a Bz increase and moderately fast earthward flow on the earthward side and a Bz decrease and fast tailward flows on the tailward side (both consistent with a plasmoid release tailward). When combined with the demonstration of a close temporal and spatial

(azimuthal) association between global auroral brightening and fast tailward flows at $r > 23$ Re [*Ieda et al.*, 2008], these results confirm that magnetic reconnection plays a major role in plasma sheet reconfiguration at substorm onset. Although the above studies indicate that plasma sheet reconnection signatures often start before auroral brightening (by 2–4 min in some cases), this result is not final given the 1–2 min time resolution of the space-based imagers used. However, the aforementioned pattern of plasma sheet reconfiguration and flows around the time of substorm onset has been corroborated by many individual case studies using THEMIS radial alignments (with spacecraft at ~11 Re, ~16 Re and ~25 Re). Many of these case studies were presented at the recent International Substorm Conference (ICS10 [see *Kissinger and McPherron*, 2010]); the proceedings were published in a special Journal of Geophysical Research volume on the topic.

[6] An important difference between these statistical studies and the previous reconnection paradigm is that the average location of reconnection is found to be closer to Earth (~18 Re) than in previous claims (20–30 Re). This is also consistent with the *Petrukovich et al.* [2009] survey of onsets made under the restriction that the Cluster spacecraft stay inside the thin current sheet (TCS) prior to onset. An extreme example of reconnection events at substorm onsets initiated as close as ~12 Re under enhanced SW dynamic pressure has been demonstrated for three consecutive breakup events observed with good coverage by Cluster, Goes, and TC-2 spacecraft using the full set of reconnection tests [*Sergeev et al.*, 2008].

2.2. Timing of Basic Substorm Onset Phenomena

[7] Substorm timing is one of the major THEMIS goals, with excellent ground ASI coverage and regular radial spacecraft conjunctions organized to meet it. A major challenge is that some basic phenomena, such as fast earthward flows, are localized within a thin portion of the plasma sheet and can easily be missed if the spacecraft stays a little outside it. *Angelopoulos et al.* [2009] recognized (and MHD simulations by *Birn et al.* [2011] supported) that in such a case, cross-field motions of plasma tubes in nearly incompressible plasma can be detected in a wider region because of the continuous nature of the reconnection electric field. Thus, flux transport is a more reliable, objective method of timing the explosive onset of magnetotail reconfiguration. Using this method, *Liu et al.* [2011a] superposed data relative to the onset of midlatitude Pi2s (as an onset time marker) for many events observed in three distance ranges during two THEMIS tail seasons. They obtained the following results: Intense flux transfer starts in the midtail (~18–30 Re) group, then ~2 min later it is observed at ~11 Re, and only ~3–4 min later is the ground Pi2 observed. Since auroral breakup typically precedes midlatitude Pi2 by roughly 0–2 min, this result suggests that auroral breakup is observed within one minute of onset signatures at ~11 Re, and that both are preceded by flux transfer onset in the midtail regions. This result is consistent with the reconnection-based onset scenario of substorms, corroborates the statistical results of *Miyashita et al.* [2009], and agrees with many tail-aligned multi-spacecraft substorm studies published in the special JGR issues on THEMIS (2010) and on substorms (2011).

[8] *Angelopoulos et al.* [2008] documented this timing sequence for two textbook cases of substorm observations made on 26 February 2008. The events were observed using ideal spacecraft conjunction and placement relative to the plasma sheet. These two events were later reanalyzed in two independent studies. *Pu et al.* [2010] confirmed the main conclusions of *Angelopoulos et al.* [2008], although with emphasis on the first of the two onsets, and *Lui* [2009] pointed out that their measurements could be interpreted differently (also see *Lui* [2011] and refutation of Lui's arguments by *Angelopoulos et al.* [2009] and *Liu et al.* [2011b]). Parallel independent analyses of the same events have revealed very clearly two remaining difficulties with the multi-spacecraft timing approach: (1) case studies are quite sensitive to spacecraft coverage (in fact, they result in indeterminacy or incorrect conclusions if spacecraft are in the wrong place) and (2) choices of essential substorm observables and thresholds used to identify local activity onset are subjective. It is therefore not surprising that by combining onset times from case studies made with different coverages and published by various authors, *Lin et al.* [2009] obtained a very noisy timing pattern. As we will see below, the emerging understanding that prevailing magnetotail conditions at substorm onset encompass sporadic excitation of localized activity suggests that timing diagrams of incoming flows may be further confounded by the presence of multiple simultaneous-activity centers. Therefore, systematic time-delay patterns as revealed by well-designed statistical studies [*Machida et al.*, 2009; *Liu et al.*, 2011a] become all the more important.

2.3. Interpretation of Auroral Breakup Observations

2.3.1. Coupling of Auroral Breakup to Flow Bursts

[9] In the following, substorm breakup is defined as explosive auroral brightening of the equatorward arc. This definition includes isolated onsets with full poleward expansion (classical substorms) as well as pseudobreakups and separate or subsequent substorm intensifications. Investigation of a database of ~250 breakup events recorded with good time resolution and coverage by the THEMIS ASI network has revealed that in most cases breakup is preceded by substantial streamer activity in the poleward region [*Nishimura et al.*, 2010; *Mende et al.*, 2011]. The streamers propagate toward the equatorward arc and are often followed by breakup near the place and time of closest approach to the equatorward pre-breakup arc. Note that streamers are often called poleward boundary intensifications (PBIs), even though PBIs may not exhibit equatorward motion. They are also referred to as North–South arcs even though streamers can often evolve in a nearly azimuthal direction both at their starting point, near the polar cap boundary, and near their ending point, close to the equatorwardmost portion of the oval.

[10] By substantiating this as the most typical sequence leading to substorm breakup, these observations have changed the substorm onset paradigm. They reveal communication between different parts of the system and the possibility that breakup is triggered by flow bursts (BBFs), and emphasize that breakup and flow bursts are initiated in different magnetospheric regions. We note that the close relationship between streamers and BBFs has strong observational support [see *Xing et al.*, 2010a, and references therein]. Therefore, the new findings from the THEMIS

ground-based observations of auroral streamer participation in the nominal substorm sequence provide clear evidence that magnetotail reconnection initiates the substorm onset process, which is consistent with our discussion on timing in 2.1 and 2.2. We caution, however, that given the uncertainty in locating the exact open-closed field line boundary by ground observations, assigning the source location of the streamers to the mid-tail or the distant tail would be unwarranted without in situ (tail) multi-spacecraft observations.

[11] The average time between the start of streamer propagation and the ensuing breakup (5 min) is consistent with timing results from in situ measurements (Sections 2.1 and 2.2). That breakup is triggered by the flow bursts is further supported by the observation that consecutive streamers may each result in local brightenings (or, in fact, progressive formation) of an equatorward, pre-breakup arc (PBA), although only the last streamer may result in classic breakup followed by poleward expansion [*Nishimura et al.*, 2011].

[12] Two issues are as yet unresolved: (1) the magnetotail preconditioning prior to onset and (2) the breakup mechanism after flow-burst arrival at the inner magnetosphere. Both remain because details of the interaction between streamers and the PBA are unresolved: where in the magnetosphere does the interaction occur; what type of interaction results in auroral signatures of breakup; and when are the flow bursts more geo-effective? A difficulty is that in white-light imaging, the auroral forms in the contact area are rather faint compared to the background. Studies using more sensitive, filtered imaging [*Kepko et al.*, 2009] show a far more complex interaction. Also, note that the last two minutes of the ~5 min time delay between the start of streamer development and the breakup correspond to the time period after streamer arrival in proximity to the prebreakup arc [*Nishimura et al.*, 2010]. In half the events, during these last 2 minutes the streamers are typically deflected azimuthally and move along the prebreakup arc. The actual motion of the magnetospheric counterparts of the flux tubes during this stage is unclear: is the flow diverted, do the flux tubes rebound, or are waves set up along the inner edge of the plasma sheet? Probably all of these phenomena are manifest, yet which one drives plasma sheet evolution, and which one corresponds to the observed emissions on the ground? These questions remain open for future investigations.

2.3.2. Breakup Mapping to the Magnetosphere

[13] Because the breakup location is near the equatorward edge of the auroral oval and poleward of but close to the peak of proton precipitation [e.g., *Donovan et al.*, 2008], it is common to place the auroral breakup's equatorial projection inside the dipolar region of the magnetotail. On the other hand, the close correlation of the breakup with midtail reconnection signatures and BBFs [e.g., *Ieda et al.*, 2008] argues in favor of tail current-sheet origin for the breakup. Resolution of this puzzle calls for accurate mapping between the ionosphere and magnetosphere. Good magnetotail coverage by THEMIS and GOES spacecraft between 6.6 and 16 Re has facilitated data-adapted magnetic field models at 1 min resolution applicable to the slowly varying conditions of the substorm growth phase (spacecraft coverage is still inadequate for reconstruction of the structured, dynamic expansion phase configuration). New magnetic field modeling tools, supported by independent, isotropy boundary analyses, allow for reconstruction of an embedded thin current sheet (TCS) as well as its north–south offsets due to solar wind velocity, etc., variations [*Kubyshkina et al.*, 2011; *Sergeev et al.*, 2011, 2012]. According to such modeling, the PBA is located from 7.5 to 9 Re (depending on the amount of tail stretching), where the magnitude of the equatorial magnetic field is as small as 5 to 20 nT, the plasma beta is high, and a strong radial magnetic field gradient exists in the presence of a thin current sheet [*Sergeev et al.*, 2012]. Just poleward of this PBA, the magnetic flux tubes project to the tail-like equatorial region where Bz is very small or possibly exhibits a local minimum not well-resolved by any model. Under such conditions, a small change/uncertainty in ionospheric latitude results in a high uncertainty in the mapped equatorial projection. Therefore, if the breakup arc forms somewhat (a few tens of kilometers) poleward of the main PBA, the breakup process may potentially be mapped to the neutral plane (Bz ≤1–2 nT) of the thin current sheet. It appears that with the number and configuration of available spacecraft, the exact breakup location in space cannot be fully resolved based on mapping techniques alone.

2.3.3. Complexity of the Auroral Breakup Process

[14] Improved instrument and network capabilities as well as careful analysis of modern, high cadence, high spatial resolution global observations have revealed that an auroral breakup is not as simple as previously thought. It is most often accompanied by PBA structuring, and major auroral brightening consists of an exponential intensity increase with a 10–30 sec e-folding time. Moreover, the arc segment that brightens extends over approximately 1 hr in MLT and features wave-like longitudinal deformations with wave numbers 100–300, such that the wavelength is comparable to the ion gyroradius in the central plasma sheet [*Donovan et al.*, 2008; *Liang et al.*, 2008]. In classical substorms, poleward expansion follows within a few minutes. Relative timing between these three stages prior to auroral expansion awaits systematic study. There is ambiguity, however, in published breakup timing results because authors have used different auroral signatures for them.

[15] Another often overlooked point of complexity concerns the role of the ionosphere. Recent and past conjugate observations reveal breakup timing differences on the order of a few minutes at opposite hemispheres [e.g., *Morioka et al.*, 2011]. These differences suggest that the auroral ionosphere may partly control auroral breakup timing. A final but significant complication in our reliance on auroral observations to study space processes is that auroral brightening is caused and modulated by a number of processes: loss-cone precipitation by waves, formation of field-aligned potential drops, and acceleration by kinetic Alfven waves. Thus, many different plasma instabilities over a large range of frequencies and spatial scales may contribute to the observed auroral structuring. It is no surprise, therefore, that there is no clear understanding of the physics, even for the quiet pre-breakup auroral arc, hindering further interpretation of auroral changes in terms of magnetospheric processes during times of active auroras.

2.4. Conditions for Instability

[16] Recent analyses [*Freeman and Morley*, 2009; *Newell and Liou*, 2011] suggest that solar wind interplanetary magnetic field triggering is not as prominent an aspect of substorms as previously envisioned. Along with results described in section 2.3., this suggests that internal

instability due to elevated solar wind driving is likely the cause of substorms. What are the conditions for such an instability?

2.4.1. Plasma Sheet Preconditioning

[17] Thin current sheets (TCS) embedded horizontally inside the near-Earth tail current sheet have previously been identified and systematically studied, most recently using Cluster. Quantitative characteristics of these embedded sheets have been discussed in the framework of embedded models [*Petrukovich et al.*, 2011]. Embedded sheets typically have scales of a few ion gyroradii, provide peak current densities of a few tens of nA/m^2 (an order of magnitude larger than nominal current sheet values), and have magnetic fields B_0 about 30–40% of the total lobe magnetic field, with the TCS outer boundaries located at a plasma beta of ~2–4. Analyzing the vertical (B/B_0-dependent) electron temperature profiles and interpreting them in the framework of adiabatic convection, *Artemyev et al.* [2011] estimated the TCS length scale to be $Lx \sim 5 - 20$ Re, with $Lx/Lz \sim 25$. They also found a typical ratio of $(2BzLx)/(BoLz) > 2$, which suggests that ion inertia along the field lines is more important than radial pressure gradients in keeping the TCS in equilibrium. Significant work has also been done analyzing the ion distribution functions in embedded thin current sheets and confirming their consistency with analytical models of these sheets, effectively enabling remote sounding of the global current sheet structure from 3D distributions on a single spacecraft [*Zhou et al.*, 2009; *Artemyev et al.*, 2010]. Such modeling, when applied in time-dependent current sheet situations and for multiple satellites, can reveal salient changes in current sheet density, pressure, magnetic field, and their gradients that are important at the late stages of the substorm growth phase.

[18] With regard to changes immediately preceding substorm onset, we now realize that plasma/current sheet thinning possibly includes two phases (or modes): gradual thinning associated with lobe magnetic pressure increase during the growth phase and fast growth of the embedded TCS at ~11 Re for ~10 minutes preceding onset, which continues without obvious increase in total pressure or convection [*Saito et al.*, 2011; *Sergeev et al.*, 2011]. Specifically, using observations from a cloud of 5 THEMIS probes, *Saito et al.* [2011] analyzed the force balance in Z and argued that such thinning is an MHD force-balanced, self-evolving process that also includes a change in the radial plasma pressure profile in the near-Earth tail. For the same event *Saito et al.* [2010] demonstrated that the Bz-component (in that case, the component normal to the TCS plane) has a pronounced minimum of <2 nT at the neutral sheet. This was associated with a configuration exhibiting a local minimum of Bz in the radial direction. Such a configuration can be quite general, because in THEMIS observations near midnight at ~11 Re, a weak B magnitude (below 1–2 nT) in the neutral sheet is fairly common prior to substorm onset, even for modest-intensity substorms. Although the *Saito et al.* [2010] conclusions require direct confirmation, significant advances in this area can be made using available spacecraft data.

2.4.2. Local or System Instability?

[19] Configurations with a minimum Bz along the downtail distance, i.e., with a tailward gradient dBz/dX, have been shown to be favorable for growth of a number of plasma instabilities, such as ballooning/interchange [e.g., *Raeder et al.*, 2010; *Pritchett and Coroniti*, 2010, 2011, and references therein], tearing [e.g., *Sitnov and Schindler*, 2010, and references therein], and MHD kink and sausage types [e.g., *Erkaev et al.*, 2008]. Not only can some of these generate signatures similar to onset (e.g., local dipolarizations or/and azimuthal structuring), but they also have been shown to stimulate fast reconnection (see, e.g., kinetic simulations by *Pritchett and Coroniti* [2011], and MHD simulations by *Birn et al.* [2011]). Recent observations from Geotail [*Saito et al.*, 2008] and THEMIS (E. V. Panov et al., Observations of kinetic ballooning/interchange instability signatures in the magnetotail, submitted to *Geophysical Research Letters*, 2012; A. Runov et al., Multi-point observations of dipolarization front formation by magnetotail reconnection, submitted to *Journal of Geophysical Research*, 2012) have indeed demonstrated both the presence of low-frequency, azimuthally-periodic perturbations in the magnetotail and their kinetic nature. Further observations of auroral waves and their westward propagation [*Liang et al.*, 2008; *Uritsky et al.*, 2009; *Rae et al.*, 2010] corroborate findings from in-situ plasma sheet measurements. Such wave-like perturbations are often observed for tens of minutes prior to breakup [*Uritsky et al.*, 2009; Panov et al., submitted manuscript, 2012], however, and therefore it is unclear whether the waves are critical in triggering an explosive onset of magnetotail instability or are a consequence of nearby, pre-onset flow bursts that have failed to initiate a substorm.

[20] In addition to localized instabilities, loss of global MHD equilibrium of the tail-like configuration is also possible [e.g., *Birn et al.*, 2009; *Sitnov and Schindler*, 2010, and references therein]. In theory and observations, such evolution should manifest as a continuum of quasi-static equilibria subject to slowly-varying (or stable) external conditions, up to a point where no self-consistent solution exists (the analytical or numerical model becomes unstable). Such instabilities may grow explosively while conserving tail-like topology and stimulate fast reconnection in their aftermath. This behavior, which has been observed in high-resolution runs of global MHD simulations [*Raeder et al.*, 2010, and references therein], implies multi-stage onset of instabilities involving finite radial and azimuthal wavenumbers. Therefore, it goes beyond the simplistic, one-dimensional In/Out substorm scenario that dominated in previous years. Such interactions between different instabilities in the large-scale magnetospheric system are difficult to study experimentally with the small number of satellites currently available (few, up to 5–7 at a time). Theoretical/simulation studies are opening up new avenues for global system destabilization; observational tests of potential paths to onset require careful multi-point correlations with fortuitous conjunctions between available satellite fleets (THEMIS, Cluster, GOES, etc.).

3. Flow Bursts and Dipolarizations

[21] Observations made by spacecraft clusters at mesoscale (~1 Re) resolution have improved our understanding of flow bursts (BBFs) and the dipolarization fronts embedded within them. Statistically, fast flow bursts observed at ~11 Re are closely correlated with substorm onsets based on the AL index [*McPherron et al.*, 2011]. They are also interesting by themselves as key elements of plasma sheet transport and injection in the closed flux tubes of the

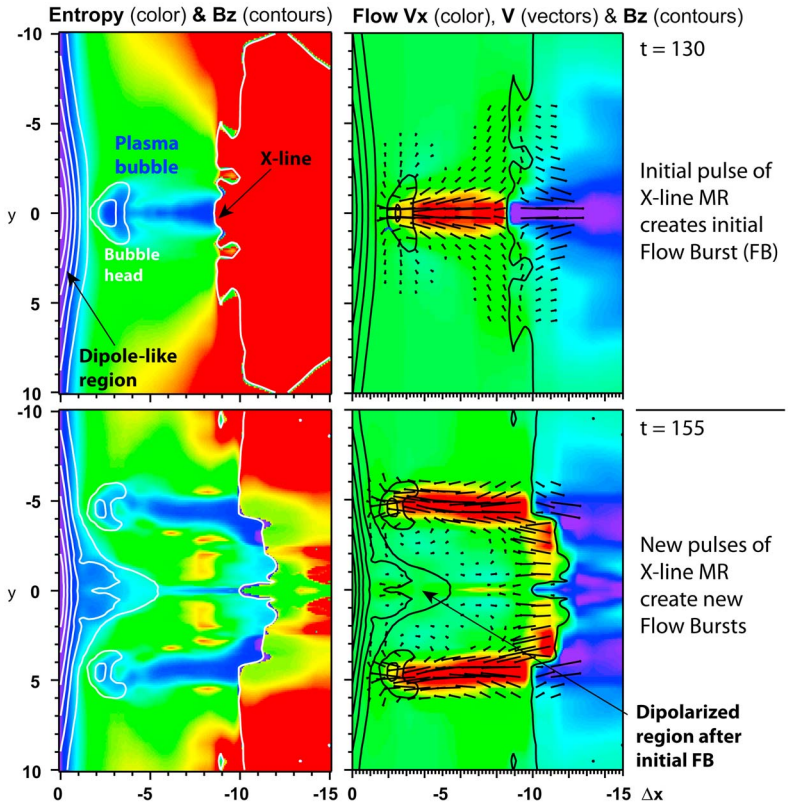

Figure 1. Equatorial view of consecutive flow bursts approaching the dipole-like region (to the left), which are formed by magnetic reconnection (MR) pulses. (top and bottom) Two simulation times separated by ~4 minutes. (left) Colored distributions of plasma tube entropy (increasing from blue to red). (right) Velocity directions (arrows) and Vx amplitudes (yellow-red colors for positive Vx, blue colors for negative Vx, green corresponds to Vx ≃ 0). Bz contours are overlain in all panels to show dipolarizations and facilitate comparisons of left- and right-side plots (adapted from *Birn et al.* [2011, Figure 8]).

magnetotail. Magnetohydrodynamic simulations of the BBF/injection process have provided an important framework for such investigations by revealing the dynamics of the global system in all its complexity [see, e.g., *Birn et al.*, 2011; *Ge et al.*, 2011; *Yang et al.*, 2011] (see Figure 1). The term dipolarization (observationally linked to increase in the magnetic field Bz component) is more broadly defined than the term flow burst, because it includes contributions from different processes, such as transient increase due to (a) flow burst passage (an intrinsic part of BBFs), (b) magnetic flux pileup (related to BBF braking and BBF interactions), and (c) global magnetospheric reconfiguration, e.g., induced by solar wind changes, etc., not related to BBFs. (See, e.g., *Nakamura et al.* [2009] for a distinction between (a) and (b) types in observations; these types are also illustrated in Figure 1.) The terms flow burst and BBF are used here interchangeably and in a general sense, with no particular threshold for time scale or flow and flux transport magnitude.

3.1. Flow-Burst Structure

[22] In-situ magnetotail observations by radially separated THEMIS spacecraft have shown that flow bursts are specific individual plasma/flow structures [e.g., *Runov et al.*, 2009] lasting several minutes and propagating predominantly earthward along the tail (as shown in Figure 1), rather than the result of random fluctuations from plasma sheet turbulence or steady convection. As discussed earlier, their coherent motion is corroborated by observations of their auroral manifestation, auroral streamers. Isolated flow bursts share a self-similar structure across large distances, encompassing a compressed magnetic field near the flow burst head (Figure 1) with a sharp dipolarization front (DF) separating the compressed ambient plasma from the newly-arriving, heated, density-depleted plasma (see, e.g., superposed epoch results by *Runov et al.* [2011]). More complicated structures are fairly common, especially near the inner magnetosphere, as expected from mutually-interacting structures and front structuring due to instabilities [*Lapenta and Bettarini et al.*, 2011, and references therein].

3.1.1. Compression Region

[23] A plasma compression region ~1 min in duration is seen both statistically and during clearly defined DF events [*Li et al.*, 2011; *Runov et al.*, 2011]. A smooth increase in the bulk flow, plasma density, and plasma pressure (up to 20–40% depending on distance) in the plasma ahead of the DF, with unchanged entropy and electron anisotropy, can be understood as plasma pileup in front of a moving body (BBF proper). At the kinetic level, the enhanced bulk flow and pressure are caused by a separate ion population superimposed on a pre-existing plasma sheet population. Particle-tracing simulations show that the observed new ion population is pre-existing plasma sheet ions that have been reflected and accelerated by the magnetic and electric fields of an approaching dipolarization front [*Zhou et al.*, 2011].

Thus, this population, initially a mere precursor of the approaching dipolarization fronts, eventually overwhelms the duskward (gradient) anisotropy of the pre-existing current sheet and is replaced smoothly by the earthward-convecting bulk flow once the dipolarization front arrives. The function of the compression region ahead of the DF, much like pressure fronts ahead of corotating interaction regions in the solar wind, is therefore to communicate the forces on the approaching front to the ambient medium. This communication, however, appears to occur in a fully kinetic manner.

3.1.2. Dipolarization Front

[24] Dipolarization fronts are localized thin current sheets of intense, approximately dawn-to-dusk-directed currents (up to several tens nA/m^2) that are often preceded by a short dip in the Bz-component [*Runov et al.*, 2009, 2011; *Sergeev et al.*, 2009; *Schmid et al.*, 2011]. Unlike the horizontal thin current sheets discussed earlier, DFs near the center of the plasma sheet are oriented normal to the neutral sheet (i.e., they lie roughly in the Y-Z plane rather than in the X–Y plane). A DF current sheet has a characteristic scale of 1–3 ion inertial (or ion gyroradius) lengths, which is, to first approximation, independent of DF propagation speed [*Schmid et al.*, 2011]. A DF is collocated with the sharp plasma boundary that separates the colder, denser ambient plasma ahead of it from the more energetic but density-depleted incoming plasma behind it. Due to its localized (ion gyroscale) and partly demagnetized ions, a DF includes a narrow region of intense earthward Hall-type E-field along its normal, it also displays a large duskward electric field along its plane [*Runov et al.*, 2011] . DFs host very strong (up to ≤100 mV/m) low-hybrid waves [*Sergeev et al.*, 2009; *Khotyaintsev et al.*, 2011] the significance and role of which are not yet understood.

[25] A few attempts have been made to analyze the currents and force balance near dipolarization fronts assuming that they have simple (locally planar) geometry. A pressure gradient of 1 to −10 keV electrons, rather than the basically diamagnetic ion current (with some electron contribution) ahead of the DF [*Zhang et al.*, 2011], was identified as a dominant contributor to the current in the dipolarization fronts. The force balance estimates of *Li et al.* [2011] showed a decrease in tailward pressure gradient force ahead of the front, suggesting earthward flow acceleration by the dominating Ampere force. Even though the radius of field line curvature increases behind the front, the curvature force density increases even further, mostly due to increase in the magnetic field magnitude. Thus, plasma acceleration at and immediately after the dipolarization front may be explained by the increased curvature force density.

[26] The nature of the dipolarization front and its role in heating the plasma behind it have not been fully resolved by observations. The observed $\mathbf{j} * \mathbf{E} > 0$ and the associated sharp increase in the energetic particle flux suggest a dissipative boundary where the plasma is locally heated [*Runov et al.*, 2011]. However, accurate computation of $\mathbf{j} * \mathbf{E}$ in the plasma frame is difficult given uncertainties in the boundary normal orientation and the temporal aliasing of the measured particle distributions at the sharp density and magnetic field front gradients. Additionally, velocities near the DFs are as small as several tens of km/s and up to 200 km/s, especially when observed within the nominal flow-braking region (inside $r \leq 11$ Re). Because these speeds are 5 to 10 times smaller than the magnetosonic speed in the plasma sheet, fast shocks are excluded. Moreover, the Bn component (the minimum variance magnetic field component, a proxy for the DF normal component) is typically very small [e.g., *Runov et al.*, 2011, Figure 7], indicating that the current layer has no magnetic field component across it. Given the uncertainties of ion flow measurements, observations of flow normal to the fronts in the front frame are, in fact, also consistent with zero, suggesting a DF resembling a non-dissipative tangential discontinuity. The curved shape of the DF in the XZ plane resembles the standard shape of a field line closing through the plasma sheet. The sharp, intense changes of energetic electron flux are hard to explain as acceleration by the measured electric fields [*Khotyaintsev et al.*, 2011]. Most of these observations suggest that the DF is a passive boundary between two distinct plasma populations rather than an active dissipative region.

[27] Although DF studies are very recent, it has been already noted that there can be different types of dipolarization fronts. In addition to the classical earthward-moving fronts, a small fraction of all DFs may propagate tailward, due to either intense flux pileup [*Nakamura et al.*, 2009; *Zhang et al.*, 2011] or rebound [*Panov et al.*, 2010b; *Schmid et al.*, 2011]. Even in the case of earthward-moving fronts, there can be different types of fronts (e.g., decaying or growing DFs, with drastically different electron acceleration properties, as has been discussed by *Fu et al.* [2011]). These structures are a fertile topic for future detailed research studies.

3.1.3. Flow Burst Proper and Related Convection Pattern

[28] A sharp (ion gyroradius scale) DF coincides with the sudden appearance of a new density-depleted, heated plasma population, enriched in energetic particle fluxes [see, e.g., *Runov et al.*, 2009, 2011]. Compared to pre-BBF plasma, this population possesses a larger local entropy ($P/n^{2/3}$) but smaller plasma tube entropy $pV^{5/3}$ and a total flux tube content depleted by ∼40% [*Dubyagin et al.*, 2010]. After a BBF passes, the plasma properties (dipolarization, heating) often persist for several minutes, as seen pictorially in Figure 1.

[29] With the help of multiple spacecraft (Cluster, THEMIS) in proximity to one another observing fast earthward flow, the flow pattern surrounding the flow burst has been discerned. Specifically, the tailward, return flows expected around the bubble edges have been identified [*Keiling et al.*, 2009a; *Walsh et al.*, 2009]. Significant evidence regarding the effects of those return flows has been obtained by combining in-situ observations with conjugate ground-based optical data plus convection as inferred from EISCAT and/or equivalent currents [see, e.g., *Keiling et al.*, 2009a, 2009b; *Pitkanen et al.*, 2011]. These studies have generally confirmed the pattern expected from field-aligned current generation around flows in the bubble theory, but have also revealed dawn-dusk asymmetries in the return flows and plasma properties that deserve further attention.

3.2. Entropy Depletion and Plasma Injections

[30] The large density depletion behind flow burst-related DFs, the general correlation of the peak flow velocity with the density depletion magnitude [*Kim et al.*, 2010], the aforementioned observations of flow vortices in the convection pattern surrounding DFs, and the tangential discontinuity nature of the DF itself (section 3.1.2) are all strong

arguments in favor of the "bubble" model of flow burst introduced by D. Pontius and R. Wolf [*Wolf et al.*, 2009, and references therein]. According to this model, the primary controller of bubble motion is the entropy parameter $S = PV^{5/3}$, which is expected to be conserved in a contracting flow-burst flux tube [*Birn et al.*, 2009]. Its gradients in the cross-tail current direction (characterizing the divergence of perpendicular cross-tail currents in the plasma tube), which are related to the polarization of the plasma tube, cause both the flow vortex and the Region-1 sense field-aligned currents to be sent to the ionosphere. The depleted plasma tube will be polarized and move earthward with respect to its neighbors until reaching the place where its entropy becomes equal to that of the ambient plasma (in the ambient plasma, S strongly increases with increasing distance in the tail, see Figure 1). Detailed MHD and RCM simulations provide a solid framework for interpreting observed details of flow-burst propagation, structuring, and flow braking in realistic configurations [see, e.g., *Birn et al.*, 2011; *Yang et al.*, 2011].

[31] Although the "bubble" model of flow burst propagation has received considerable observational support, significant complications arise with how to estimate a non-local parameter, the volume of a unit flux tube ($V = \int ds/B$), using local measurements. *Wolf et al.* [2006] suggested an approximate formula to compute V from single spacecraft observations by averaging results of many equilibrated models. The performance of this model has been independently tested against MHD simulations [*Birn et al.*, 2011]. Using this tool, *Dubyagin et al.* [2010] showed systematic entropy depletions in the wake of dipolarizations in the flow-braking region (6–12 Re) relative to conditions prior to flow burst arrival. Entropy changes brought about by incoming flow bursts show a statistically significant decrease relative to ambient conditions with proximity to Earth; this behavior continues as close to Earth as the geostationary altitude. By comparing observations of radially-separated THEMIS spacecraft, *Dubyagin et al.* [2011] confirmed the capability of the bubble model to predict energetic particle increase at the inner spacecraft (at ~9 Re) based on the difference between ambient entropy there and the minimum entropy in the flow burst recorded at the outer spacecraft (~11 Re).

[32] These results clarify why individual flow bursts differ in their geo-effectiveness (their ability to inject plasma into the inner magnetosphere); the defining property is entropy within the plasma tubes of the flow. Using superposed epoch analyses of flow bursts in Geotail observations, *Yang et al.* [2010] showed a systematic entropy decrease as well as a progressively larger entropy depletion from pre-onset conditions when examining pseudo-breakups, substorms, and SMC events, correspondingly. The same principle helps us understand that the potential for plasma injection (and dipolarization) to a specific earthward distance (e.g., to geostationary orbit) also depends on the ambient value of plasma tube entropy at that location prior to injection (i.e., on the color at the observation point on the left-side of Figure 1). This value varies considerably with the amount of magnetic field stretching in the magnetotail. This simple scheme of predicting the penetration depth based on the bubble entropy S needs to be modified by the violation of plasma tube entropy conservation in the inner magnetosphere due to diamagnetic drifts (and possibly other factors, such as turbulent mixing). These aspects have yet to be addressed quantitatively.

[33] Although the basic mechanism that creates plasma-depleted flux tubes (bubbles) is magnetic reconnection [*Wolf et al.*, 2009; *Birn et al.*, 2011], modestly-depleted bubbles might be formed in interchange-unstable regions of the plasma sheet (such as the region of tailward dBz/dX gradients, tailward of a local B-minimum, as discussed, e.g., by *Pritchett and Coroniti* [2011]). The latter mechanism, however, still awaits observational confirmation. Nevertheless, it is unlikely that an interchange process operating on closed tubes at r < 15–20 Re would be capable of producing significant entropy depletions given the already large-entropy plasma contained in flux tubes at such distances. Therefore, recent observations of strongly underpopulated plasma bubbles could be considered indirect confirmation of the magnetic reconnection process operating further downtail, and further quantitative confirmation of that hypothesis from radially separated spacecraft would provide significant impetus to substorm research.

3.3. Flow-Burst Braking and Diversion

[34] The braking of fast plasma flow coming from the tail, its inward penetration, and/or its diversion around the inner magnetosphere are among the basic processes/elements of magnetospheric circulation. With the availability of THEMIS spacecraft to monitor distances on the order of several ion gyroradii up to the scale size of flows and pressure gradients, the spatio-temporal flow pattern surrounding flow bursts has begun to be elucidated. For example, it was demonstrated that entry of a flow burst (transient dipolarization pulse) into the inner magnetosphere is accompanied by growth in total plasma pressure [*Dubyagin et al.*, 2010; *Xing et al.*, 2010b], whereas the increase (or relaxation) of the radial pressure gradient was shown to be associated with flow stoppage (or rebound) [*Panov et al.*, 2010a].

[35] Statistical results also confirm that in dipolarization events, initial flow-burst intrusion and increased radial pressure gradients are typically followed by tailward motion on closed magnetic tubes [*Ohtani et al.*, 2009]. The return flows are sometimes observed over a wider region than initial earthward flows seen pictorially in Figure 1. In the magnetotail such flows are statistically observed over a 4 hr-wide region in MLT, centered at 23.5 hr MLT [*McPherron et al.*, 2011]. At this stage, a tailward-progressing dipolarization (related to flux pileup) is seen tailward of the flow-braking region [*Nakamura et al.*, 2009; *Zhang et al.*, 2011] (also see Figure 1, bottom). Flow-burst stoppage may include multiple overshoots and associated flux tube oscillations around an equilibrium point [*Wolf et al.*, 2009]. Similar oscillatory motions with ~2 min time periodicity have been indeed captured in THEMIS observations [*Panov et al.*, 2010b]. Such multi-spacecraft observations document complicated flow patterns during flow bursts which, to a first approximation, seem to conform to a paradigm of medium (a few Re)-scale flow vortices (although even the modern spacecraft clusters still have rather sparse coverage). So far, most reported THEMIS observations [e.g., *Keiling et al.*, 2009a; *Panov et al.*, 2010a, 2010b] have been done near the flow-braking region, as in Figure 1, where the vortex flow pattern looks most pronounced in the MHD simulations. At many points these initial important observations

need to be complemented by more systematic studies at other distances as well as statistical studies.

[36] Recent observations of flow-burst rebound and oscillatory long-term evolution, and particularly the complex interaction between flow bursts and large-scale dipolarization, bring us to new topics. The actual magnetotail system displays multiple activity centers and multiple activity pulses (multiple flow bursts), so interaction of different flow bursts with each other and with the expanding large-scale dipolarization in the inner magnetosphere is unavoidable when explaining the dynamics of substorm expansion phase and recovery. High-resolution MHD simulations already provide a hint of the complexity and variability of flow-burst interactions [e.g., *Ge et al.*, 2011]. A related aspect of the system-wide evolution is the diversion and fragmentation of propagating flow bursts. Finally, the concurrent evolution of micro- and meso-scale instabilities may play a significant role in particle heating and also affect flow-burst evolution (see, e.g., *Lapenta and Bettarini* [2011] for simulations and *Hwang et al.* [2011] for observations).

4. Summary

[37] Recent observations by greatly improved space and ground networks as well as comprehensive statistical studies have enabled significant advances in our understanding of magnetotail dynamics around substorm onset. Observations confirm that midtail reconnection is closely associated with auroral breakup and substorm onset. It typically starts a few minutes prior to auroral breakup (statistically at around 18 Re, with many examples starting closer to the Earth), initiates flow bursts (BBF), and is the major driver of the substorm expansion phase – that is, the major energy dissipation and current disruption (unloading) process. Prior to onset, large-scale reconfiguration of the tail current sheet takes place simultaneously with local instabilities, which may interact with each other and even develop explosively, leading to onset. Such multi-scale disturbances could result in a complex observational environment that may include multiple paths to onset. Such internal processes may additionally depend on solar wind conditions and activity history, which were not discussed in the present paper due to space limitations. The substorm onset process is therefore an area of active research requiring a system-wide approach and close interaction among theory, data analysis, and simulations.

[38] The following recent observations of the substorm expansion phase onset provide key information for understanding substorms and open up new directions for further advances:

1. Prior to breakup, typical auroral features (streamers) suggest BBF/flow-burst activity initiated by magnetotail reconnection. The flow bursts approaching the inner magnetosphere may influence parameters in the outer portion of the dipole-like region, causing auroral breakup. Further details of this interaction require more systematic observations and modelling studies.

2. Auroral breakup, which usually consists of structuring, explosive brightening of the equatorward arc, and then auroral expansion, likely maps to the near-Earth region. It occurs in the high-beta plasma sheet (where $B < 5 - 20$ nT) at the junction of the thin current sheet and the outer part of the dipole-like configuration. To unravel the nature of breakup-related instabilities along with the origin of azimuthal structuring and explosive brightening inferred from auroral measurements, one needs to combine conjugate auroral and spacecraft observations under the guidance of simulation models.

3. Magnetotail preconditioning seems to include two modes of current sheet thinning: (a) modest thinning/intensification during the growth phase associated with a lobe field increase and (b) reconfiguration with rapid growth of an embedded current sheet during the last ten minutes before breakup. Evidence is mounting that prior to auroral breakup, a configuration may form with a local Bz minimum (roughly at ~12 Re), which is known to be unstable to various plasma instabilities. Quantitative information from models is required to confirm this condition, describe the resultant configuration, and to identify the important wave modes that may be driven unstable in that configuration.

4. BBF/flow bursts are confirmed to contain plasma-depleted, dipolarized, fast-flow channels (plasma "bubbles") with distinct flow patterns and embedded particle populations separated from the ambient plasma by a sharp frontside boundary. The minimum value of the unit flux-tube entropy $pV^{5/3}$ in the bubble could be a predictor of flow penetration distance and associated particle injection. Flow braking and associated rebound, overshoot, and oscillations have been observed. The process by which flow bursts originate, the factors controlling flow-burst cross-tail size, the details of flow-burst diversions and interactions, flow-burst structuring due to plasma instabilities, and the role of the dipolarization front in plasma acceleration and injection are important for understanding the physics and implications of flow bursts for substorms as well as for plasma injection into the inner magnetosphere.

[39] A unique opportunity is the combination of MMS (able to monitor tail reconnection and electron kinetic physics), THEMIS and CLUSTER (able to monitor flow-burst propagation and scale size), ARTEMIS (able to monitor mid-tail reconnection region), and RBSP and other planned inner-magnetospheric missions in the years to come. Such programs, especially when intensively supported by modeling, hold great promise for resolving many of the micro- and meso- scale questions mentioned above. A global view of substorms is still elusive, however. To truly address the multi-scale magnetic field, pressure, and flow configuration changes developing during substorms, better and more numerous measurements (an order of magnitude more points, still judiciously distributed in key regions) in close conjunction with advanced modeling are required. This remains a challenge for the next generation of experimental space physicists.

[40] **Acknowledgments.** We thank Judy Hohl and E. Masongsong for help in preparing the paper, and J. Birn for providing original figure from his paper. The work was supported by EU FP7 grant 269198 (Geoplasmas), by SPbU grant 11.38.47.2011, by FWF project I429-N16 as well as by THEMIS contract NAS5-02099.

[41] The Editor thanks Larry Kepko and Joachim Birn for their assistance in evaluating this paper.

References

Angelopoulos, V., et al. (2008), Tail reconnection triggering substorm onset, *Science*, *321*, 931, doi:10.1126/science.1160495.

Angelopoulos, V., et al. (2009), Response to comment on "Tail reconnection triggering substorm onset," *Science*, *324*, 1391, doi:10.1126/science.1168045.

Artemyev, A. V., A. A. Petrukovich, R. Nakamura, and L. M. Zelenyi (2010), Proton velocity distribution in thin current sheets: Cluster observations and theory of transient trajectories, *J. Geophys. Res.*, *115*, A12255, doi:10.1029/2010JA015702.

Artemyev, A. V., L. M. Zelenyi, A. A. Petrukovich, and R. Nakamura (2011), Hot electrons as tracers of large-scale structure of magnetotail current sheets, *Geophys. Res. Lett.*, *38*, L14102, doi:10.1029/2011GL047979.

Birn, J., M. Hesse, K. Schindler, and S. Zaharia (2009), Role of entropy in magnetotail dynamics, *J. Geophys. Res.*, *114*, A00D03, doi:10.1029/2008JA014015.

Birn, J., R. Nakamura, E. V. Panov, and M. Hesse (2011), Bursty bulk flows and dipolarization in MHD simulations of magnetotail reconnection, *J. Geophys. Res.*, *116*, A01210, doi:10.1029/2010JA016083.

Donovan, E., et al. (2008), Simultaneous THEMIS in situ and auroral observations of a small substorm, *Geophys. Res. Lett.*, *35*, L17S18, doi:10.1029/2008GL033794.

Dubyagin, S., V. Sergeev, S. Apatenkov, V. Angelopoulos, R. Nakamura, J. McFadden, D. Larson, and J. Bonnell (2010), Pressure and entropy changes in the flow-braking region during magnetic field dipolarization, *J. Geophys. Res.*, *115*, A10225, doi:10.1029/2010JA015625.

Dubyagin, S., V. Sergeev, S. Apatenkov, V. Angelopoulos, A. Runov, R. Nakamura, W. Baumjohann, J. McFadden, and D. Larson (2011), Can flow bursts penetrate into the inner magnetosphere?, *Geophys. Res. Lett.*, *38*, L08102, doi:10.1029/2011GL047016.

Erkaev, N. V., V. S. Semenov, and H. K. Biernat (2008), Magnetic double gradient mechanism for flapping oscillations of a current sheet, *Geophys. Res. Lett.*, *35*, L02111, doi:10.1029/2007GL032277.

Freeman, M. P., and S. K. Morley (2009), No evidence for externally triggered substorms based on superposed epoch analysis of IMF Bz, *Geophys. Res. Lett.*, *36*, L21101, doi:10.1029/2009GL040621.

Fu, H. S., Y. V. Khotyaintsev, M. André, and A. Vaivads (2011), Fermi and betatron acceleration of suprathermal electrons behind dipolarization fronts, *Geophys. Res. Lett.*, *38*, L16104, doi:10.1029/2011GL048528.

Ge, Y. S., J. Raeder, V. Angelopoulos, M. L. Gilson, and A. Runov (2011), Interaction of dipolarization fronts within multiple bursty bulk flows in global MHD simulations of a substorm on 27 February 2009, *J. Geophys. Res.*, *116*, A00I23, doi:10.1029/2010JA015758.

Hwang, K.-J., M. L. Goldstein, E. Lee, and J. S. Pickett (2011), Cluster observations of multiple dipolarization fronts, *J. Geophys. Res.*, *116*, A00I32, doi:10.1029/2010JA015742.

Ieda, A., et al. (2008), Longitudinal association between magnetotail reconnection and auroral breakup based on Geotail and Polar observations, *J. Geophys. Res.*, *113*, A08207, doi:10.1029/2008JA013127.

Keiling, A., et al. (2009a), Substorm current wedge driven by plasma flow vortices: THEMIS observations, *J. Geophys. Res.*, *114*, A00C22, doi:10.1029/2009JA014114.

Keiling, A., et al. (2009b), THEMIS ground-space observations during the development of auroral spirals, *Ann. Geophys.*, *27*, 4317.

Kepko, L., E. Spanswick, V. Angelopoulos, E. Donovan, J. McFadden, K.-H. Glassmeier, J. Raeder, and H. J. Singer (2009), Equatorward moving auroral signatures of a flow burst observed prior to auroral onset, *Geophys. Res. Lett.*, *36*, L24104, doi:10.1029/2009GL041476.

Khotyaintsev, Y. V., et al. (2011), Plasma jet braking: Energy dissipation and nonadiabatic electrons, *Phys. Rev. Lett.*, *106*, 165001, doi:10.1103/PhysRevLett.106.165001.

Kim, H.-S., D.-Y. Lee, S.-I. Ohtani, E.-S. Lee, and B.-H. Ahn (2010), Some statistical properties of flow bursts in the magnetotail, *J. Geophys. Res.*, *115*, A12229, doi:10.1029/2009JA015173.

Kissinger, J., and R. L. McPherron (2010), A bright future for substorms: Tenth International Conference on Substorms; San Luis Obispo, California, 22–26 March 2010, *Eos Trans. AGU*, *91*(38), 335, doi:10.1029/2010EO380006.

Kubyshkina, M., V. Sergeev, N. Tsyganenko, V. Angelopoulos, A. Runov, E. Donovan, H. Singer, U. Auster, and W. Baumjohann (2011), Time-dependent magnetospheric configuration and breakup mapping during a substorm, *J. Geophys. Res.*, *116*, A00I27, doi:10.1029/2010JA015882.

Lapenta, G., and L. Bettarini (2011), Self-consistent seeding of the interchange instability in dipolarization fronts, *Geophys. Res. Lett.*, *38*, L11102, doi:10.1029/2011GL047742.

Li, S.-S., V. Angelopoulos, A. Runov, X.-Z. Zhou, J. McFadden, D. Larson, J. Bonnell, and U. Auster (2011), On the force balance around dipolarization fronts within bursty bulk flows, *J. Geophys. Res.*, *116*, A00I35, doi:10.1029/2010JA015884.

Liang, J., E. F. Donovan, W. W. Liu, B. Jackel, M. Syrjäsuo, S. B. Mende, H. U. Frey, V. Angelopoulos, and M. Connors (2008), Intensification of preexisting auroral arc at substorm expansion phase onset: Wave-like disruption during the first tens of seconds, *Geophys. Res. Lett.*, *35*, L17S19, doi:10.1029/2008GL033666.

Lin, N., H. U. Frey, S. B. Mende, F. S. Mozer, R. L. Lysak, Y. Song, and V. Angelopoulos (2009), Statistical study of substorm timing sequence, *J. Geophys. Res.*, *114*, A12204, doi:10.1029/2009JA014381.

Liu, J., C. Gabrielse, V. Angelopoulos, N. A. Frissell, L. R. Lyons, J. P. McFadden, J. Bonnell, and K. H. Glassmeier (2011a), Superposed epoch analysis of magnetotail flux transport during substorms observed by THEMIS, *J. Geophys. Res.*, *116*, A00I29, doi:10.1029/2010JA015886.

Liu, J., V. Angelopoulos, M. Kubyshkina, J. McFadden, K.-H. Glassmeier, and C. T. Russell (2011b), Revised timing and onset location of two isolated substorms observed by Time History of Events and Macroscale Interactions During Substorms (THEMIS), *J. Geophys. Res.*, *116*, A00I17, doi:10.1029/2010JA015877.

Lui, A. T. Y. (2009), Comment on "Tail reconnection triggering substorm onset," *Science*, *325*, 1391, doi:10.1126/science.1167726.

Lui, A. T. Y. (2011), Revisiting Time History of Events and Macroscale Interactions during Substorms (THEMIS) substorm events implying magnetic reconnection as the substorm trigger, *J. Geophys. Res.*, *116*, A03211, doi:10.1029/2010JA016078.

Machida, S., et al. (2009), Statistical visualization of the Earth's magnetotail based on Geotail data and the implied substorm model, *Ann. Geophys.*, *27*, 1035.

McPherron, R. L., T.-S. Hsu, J. Kissinger, X. Chu, and V. Angelopoulos (2011), Characteristics of plasma flows at the inner edge of the plasma sheet, *J. Geophys. Res.*, *116*, A00I33, doi:10.1029/2010JA015923.

Mende, S. B., H. U. Frey, V. Angelopoulos, and Y. Nishimura (2011), Substorm triggering by poleward boundary intensification and related equatorward propagation, *J. Geophys. Res.*, *116*, A00I31, doi:10.1029/2010JA015733.

Miyashita, Y., et al. (2009), A state-of-the-art picture of substorm-associated evolution of the near-Earth magnetotail obtained from superposed epoch analysis, *J. Geophys. Res.*, *114*, A01211, doi:10.1029/2008JA013225.

Morioka, A., et al. (2011), On the simultaneity of substorm onset between two hemispheres, *J. Geophys. Res.*, *116*, A04211, doi:10.1029/2010JA016174.

Nakamura et al. (2009), Evolution of dipolarization in the near-Earth current sheet induced by Earthward rapid flux transport, *Ann. Geophys.*, *27*, 1743.

Newell, P. T., and K. Liou (2011), Solar wind driving and substorm triggering, *J. Geophys. Res.*, *116*, A03229, doi:10.1029/2010JA016139.

Nishimura, Y., L. Lyons, S. Zou, V. Angelopoulos, and S. Mende (2010), Substorm triggering by new plasma intrusion: THEMIS all-sky imager observations, *J. Geophys. Res.*, *115*, A07222, doi:10.1029/2009JA015166.

Nishimura, Y., L. R. Lyons, V. Angelopoulos, T. Kikuchi, S. Zou, and S. B. Mende (2011), Relations between multiple auroral streamers, pre-onset thin arc formation, and substorm auroral onset, *J. Geophys. Res.*, *116*, A09214, doi:10.1029/2011JA016768.

Ohtani, S., Y. Miyashita, H. Singer, and T. Mukai (2009), Tailward flows with positive B_z in the near-Earth plasma sheet, *J. Geophys. Res.*, *114*, A06218, doi:10.1029/2009JA014159.

Panov, E. V., et al. (2010a), Plasma sheet thickness during a bursty bulk flow reversal, *J. Geophys. Res.*, *115*, A05213, doi:10.1029/2009JA014743.

Panov, E. V., et al. (2010b), Multiple overshoot and rebound of a bursty bulk flow, *Geophys. Res. Lett.*, *37*, L08103, doi:10.1029/2009GL041971.

Petrukovich, A. A., W. Baumjohann, R. Nakamura, and H. Rème (2009), Tailward and earthward flow onsets observed by Cluster in a thin current sheet, *J. Geophys. Res.*, *114*, A09203, doi:10.1029/2009JA014064.

Petrukovich, A. A., A. V. Artemyev, H. V. Malova, V. Y. Popov, R. Nakamura, and L. M. Zelenyi (2011), Embedded current sheets in the Earth's magnetotail, *J. Geophys. Res.*, *116*, A00I25, doi:10.1029/2010JA015749.

Pitkanen, T., et al. (2011), EISCAT-Cluster observations of quiet-time near-Earth magnetotail fast flows and their signatures in the ionosphere, *Ann. Geophys.*, *29*, 299, doi:10.5194/angeo-29-299-2011.

Pritchett, P. L., and F. V. Coroniti (2010), A kinetic ballooning/interchange instability in the magnetotail, *J. Geophys. Res.*, *115*, A06301, doi:10.1029/2009JA014752.

Pritchett, P. L., and F. V. Coroniti (2011), Plasma sheet disruption by interchange-generated flow intrusions, *Geophys. Res. Lett.*, *38*, L10102, doi:10.1029/2011GL047527.

Pu, Z. Y., et al. (2010), THEMIS observations of substorms on 26 February 2008 initiated by magnetotail reconnection, *J. Geophys. Res.*, *115*, A02212, doi:10.1029/2009JA014217.

Rae, I. J., C. E. J. Watt, I. R. Mann, K. R. Murphy, J. C. Samson, K. Kabin, and V. Angelopoulos (2010), Optical characterization of the growth and

spatial structure of a substorm onset arc, *J. Geophys. Res.*, *115*, A10222, doi:10.1029/2010JA015376.

Raeder, J., P. Zhu, Y. Ge, and G. Siscoe (2010), Open Geospace General Circulation Model simulation of a substorm: Axial tail instability and ballooning mode preceding substorm onset, *J. Geophys. Res.*, *115*, A00I16, doi:10.1029/2010JA015876.

Runov, A., V. Angelopoulos, M. I. Sitnov, V. A. Sergeev, J. Bonnell, J. P. McFadden, D. Larson, K.-H. Glassmeier, and U. Auster (2009), THEMIS observations of an earthward-propagating dipolarization front, *Geophys. Res. Lett.*, *36*, L14106, doi:10.1029/2009GL038980.

Runov, A., V. Angelopoulos, X.-Z. Zhou, X.-J. Zhang, S. Li, F. Plaschke, and J. Bonnell (2011), A THEMIS multicase study of dipolarization fronts in the magnetotail plasma sheet, *J. Geophys. Res.*, *116*, A05216, doi:10.1029/2010JA016316.

Saito, M. H., Y. Miyashita, M. Fujimoto, I. Shinohara, Y. Saito, K. Liou, and T. Mukai (2008), Ballooning mode waves prior to substorm-associated dipolarizations: Geotail observations, *Geophys. Res. Lett.*, *35*, L07103, doi:10.1029/2008GL033269.

Saito, M. H., L.-N. Hau, C.-C. Hung, Y.-T. Lai, and Y.-C. Chou (2010), Spatial profile of magnetic field in the near-Earth plasma sheet prior to dipolarization by THEMIS: Feature of minimum B, *Geophys. Res. Lett.*, *37*, L08106, doi:10.1029/2010GL042813.

Saito, M. H., D. Fairfield, G. Le, L.-N. Hau, V. Angelopoulos, J. P. McFadden, U. Auster, J. W. Bonnell, and D. Larson (2011), Structure, force balance, and evolution of incompressible cross-tail current sheet thinning, *J. Geophys. Res.*, *116*, A10217, doi:10.1029/2011JA016654.

Schmid, D., et al. (2011), A statistical and event study of magnetotail dipolarization fronts, *Ann. Geophys.*, *29*, 1537.

Sergeev, V., et al. (2008), Study of near-Earth reconnection events with Cluster and Double Star, *J. Geophys. Res.*, *113*, A07S36, doi:10.1029/2007JA012902.

Sergeev, V., V. Angelopoulos, S. Apatenkov, J. Bonnell, R. Ergun, R. Nakamura, J. McFadden, D. Larson, and A. Runov (2009), Kinetic structure of the sharp injection/dipolarization front in the flow-braking region, *Geophys. Res. Lett.*, *36*, L21105, doi:10.1029/2009GL040658.

Sergeev, V., V. Angelopoulos, M. Kubyshkina, E. Donovan, X.-Z. Zhou, A. Runov, H. Singer, J. McFadden, and R. Nakamura (2011), Substorm growth and expansion onset as observed with ideal ground-spacecraft THEMIS coverage, *J. Geophys. Res.*, *116*, A00I26, doi:10.1029/2010JA015689.

Sergeev, V., Y. Nishimura, M. Kubyshkina, V. Angelopoulos, R. Nakamura, and H. Singer (2012), Magnetospheric location of the equatorward pre-breakup arc, *J. Geophys. Res.*, *117*, A01212, doi:10.1029/2011JA017154.

Sitnov, M. I., and K. Schindler (2010), Tearing stability of a multiscale magnetotail current sheet, *Geophys. Res. Lett.*, *37*, L08102, doi:10.1029/2010GL042961.

Uritsky, V. M., J. Liang, E. Donovan, E. Spanswick, D. Knudsen, W. Liu, J. Bonnell, and K. H. Glassmeier (2009), Longitudinally propagating arc wave in the pre-onset optical aurora, *Geophys. Res. Lett.*, *36*, L21103, doi:10.1029/2009GL040777.

Walsh, A. P., et al. (2009), Cluster and Double Star multipoint observations of a plasma bubble, *Ann. Geophys.*, *27*, 725.

Wolf, R. A., V. Kumar, F. R. Toffoletto, G. M. Erickson, A. M. Savoie, C. X. Chen, and C. L. Lemon (2006), Estimating local plasma sheet PV 5/3 from single-spacecraft measurements, *J. Geophys. Res.*, *111*, A12218, doi:10.1029/2006JA012010.

Wolf, R. A., Y. Wan, X. Xing, J.-C. Zhang, and S. Sazykin (2009), Entropy and plasma sheet transport, *J. Geophys. Res.*, *114*, A00D05, doi:10.1029/2009JA014044.

Xing, X., L. Lyons, Y. Nishimura, V. Angelopoulos, D. Larson, C. Carlson, J. Bonnell, and U. Auster (2010a), Substorm onset by new plasma intrusion: THEMIS spacecraft observations, *J. Geophys. Res.*, *115*, A10246, doi:10.1029/2010JA015528.

Xing, X., L. R. Lyons, V. Angelopoulos, D. Larson, C. Carlson, A. Runov, and U. Auster (2010b), Plasma sheet pressure evolution related to substorms, *J. Geophys. Res.*, *115*, A01212, doi:10.1029/2009JA014315.

Yang, J., F. R. Toffoletto, G. M. Erickson, and R. A. Wolf (2010), Superposed epoch study of PV5/3 during substorms, pseudobreakups and convection bays, *Geophys. Res. Lett.*, *37*, L07102, doi:10.1029/2010GL042811.

Yang, J., F. R. Toffoletto, R. A. Wolf, and S. Sazykin (2011), RCM-E simulation of ion acceleration during an idealized plasma sheet bubble injection, *J. Geophys. Res.*, *116*, A05207, doi:10.1029/2010JA016346.

Zhang, X.-J., V. Angelopoulos, A. Runov, X.-Z. Zhou, J. Bonnell, J. P. McFadden, D. Larson, and U. Auster (2011), Current carriers near dipolarization fronts in the magnetotail: A THEMIS event study, *J. Geophys. Res.*, *116*, A00I20, doi:10.1029/2010JA015885.

Zhou, X.-Z., V. Angelopoulos, A. Runov, M. I. Sitnov, Q.-G. Zong, and Z. Y. Pu (2009), Ion distributions near the reconnection sites: Comparison between simulations and THEMIS observations, *J. Geophys. Res.*, *114*, A12211, doi:10.1029/2009JA014614.

Zhou, X.-Z., V. Angelopoulos, V. A. Sergeev, and A. Runov (2011), On the nature of precursor flows upstream of advancing dipolarization fronts, *J. Geophys. Res.*, *116*, A03222, doi:10.1029/2010JA016165.

V. Angelopoulos, Department of Earth and Space Sciences, University of California, 3845 Slichter Hall, Los Angeles, CA 90095-1567, USA.

R. Nakamura, Space Research Institute, Austrian Academy of Sciences, Schmiedlstraße 6, A-8042 Graz, Austria.

V. A. Sergeev, Earth Physics Department, St. Petersburg State University, Ulyanovskaya 1, Petrodvoretz, St. Petersburg 198504, Russia. (victor@geo.phys.spbu.ru)